Int J Adv Manuf Technol (2017) 90:2827–2837
DOI 10.1007/s00170-016-9586-0

ORIGINAL ARTICLE

Friction spot stir welding of polymers: control of plunging force

F. Lambiase[1,2,3] · A. Paoletti[1,2] · A. Di Ilio[1,2]

Received: 13 August 2016 / Accepted: 10 October 2016 / Published online: 22 October 2016

Abstract This study investigates the influence of the plunging force in friction spot stir welding of polycarbonate sheets on the mechanical behavior of the welds. Experimental tests were carried out by varying the tool geometry and the applied plunging force. Mechanical tests based on single-lap shear tests were carried out for mechanical characterization of the welds. Thus, the morphology of the welds was analyzed to clarify the influence of the plunging force on geometry and defects of the welds. According to the achieved results, the control of the plunging force allows improving the mechanical behavior of the welds up to 37 % without requiring for additional energy during the welding process or affecting the process production time. The increase of the weld strength is due to the reduction of porosities developing at the interface between the stirred zone and the surrounding material. However, excessive plunging force results in weaker welds due to excessive thinning of the punch-sided sheet. Under optimal conditions, the shear strength of the welds was 34.5 MPa that yields that of the base material.

Keywords Friction stir welding · Friction spot stir welding · Welding · Polymers · Material testing · Thermoplastic · Joining · Force control · Plunging force

✉ F. Lambiase
francesco.lambiase@univaq.it

[1] Department of Industrial and Information Engineering and Economics, University of L'Aquila, Via G. Gronchi 18, Zona Industriale di Pile, 67100 L'Aquila, Italy

[2] CIRTIBS Research Centre, University of Naples Federico II, P.le Tecchio 80, 80125 Naples, Italy

[3] Monteluco di Roio, 67040 L'Aquila, Italy

1 Introduction

The wide employment of lightweight structures in transportation industries is aimed at reducing vehicles weight, fuel consumption, and consequently improving the overall performances. To this end, materials other than metals such as polymers and reinforced polymers are being increasingly adopted due to their high strength-to-weight ratio. However, joining such materials requires special processes in order to prevent from stress concentration, to improve static and dynamic behavior, and to avoid material damage and distortions.

Different processes are available for joining thermoplastics including hot gas welding, speed tip welding, extrusion welding, hot plate welding, induction welding, injection welding, ultrasonic welding, friction welding, solvent welding, adhesive bonding, and mechanical fastening. However, these processes involve inefficient use of (welding) energy, specialized workers, significant environmental impact, surface pre-cleaning, etc. Thus, in the recent years, a number of newer processes have been developed based on combined thermo-mechanical joining including friction spot joining, friction-based staking, and laser welding. Friction spot joining [25] allows to easily weld metal parts to polymers by heating the metal part by friction by means of a simple rotating tool. The process exploits the thermal conductivity of the metal part to let the frictional heat diffuse towards the metal-polymer interface allowing the achievement of welding. However, this process involves more difficulties for welding polymer-to-polymer since low thermal conductivity of thermoplastics as compared to metals. Friction-based stacking requires extensive pre-working on the parts being joined: drilling a hole in the upper part and the presence of a stud, which will be thermoformed by means of a rotating tool [1], in the other part. Laser transmission welding (LTW) and laser-assisted direct joining (LADJ)

represent suitable processes when used to weld polymers and metals to polymers, such as polycarbonate [2]; however, these processes show some limitations. Actually, they require the upper polymer being transparent to the laser radiation and the lower part being absorbing the laser [12]. Thus, a lower transparent thermoplastic sheet requires additional pre-working, such as covering the bottom sheet surface by means of absorbing particles such as carbon black [3] either carbon nanotubes [22], to allow the laser radiation being absorbed.

On the other hand, friction stir-based (FSB) processes such as friction stir welding (FSW) and friction spot stir welding (FSSW) produce high strength welds, require low energy absorption, and involve low environmental impact. In addition, such processes are characterized by high reliability and robustness and do not require pre-cleaning of substrates [17]. FSB welds show restricted heating regions, which lead to higher efficiency and reduced heat affected zone and low thermal distortions and mechanical behavior comparable to those achieved by other welding processes [19] even close to the strength of the base material.

During these processes, the materials being joined are stirred by a rotating tool (with a relatively simple geometry) that translates along the weld seam (FSW) or simply plunges two overlapping sheets (FSSW). The geometry of the tool and the process parameters, including the tool rotation speed, plunging depth, and interaction time, determines the weld quality and strength. Since the heat is produced by friction work, the contact surface and the tool geometry play a crucial role on the process quality [23]. In FSSW process of PC sheets, smaller shoulder diameters are preferable to larger ones, because these welds show higher specific strength and more repeatable and more gradual failure behavior [15]. In addition, larger tools require higher welding energy [14] and produce lower strength welds with more unpredictable failure behavior.

In FSW and FSSW welds, the quality depends on the stirring and upsetting action, as well as temperature distribution. The amount of (frictional) heat transferred to the material depends on the combination of the processing conditions. In FSW, the amount of frictional heat depends on the tool rotational speed, feed rate, and tilt angle; on the other hand, in FSSW, the amount of frictional heat is determined by on the tool rotational speed, plunging speed, pre-heating time, and stirring time. Several researches were carried out to understand how the processing conditions influence the quality and strength of these types of welds. The weld strength is highly affected by the tool rotation speed, n, indeed, low value of n results in under-heating conditions, and poor material mixing. On the other hand, excessively high values of n produce excessive material softening that yields a reduction in the friction generated and reduced upsetting action [20]. Thus, the strength of FSSW and FSW welds shows a peak for the tool rotation speed as reported in [10, 11]. The weld area increases with the stirring time after reaching a plafond; this is due to higher frictional heat transferred to the material [6].

A number of studies were focused on the process enhancement by introducing some changes to the basic process scheme including control of the plunging force during FSW [16] either the employment of materials at the interface between the sheet being joined, such as multi-walled carbon nanotubes [8, 9].

New types of tools were developed including "self-retracting tool" to avoid the back slit defect [21] and tools with fixed shoulders (in FSW) [24]. The latter type of tool allows to perform a better upsetting action on the material. Indeed, when conventional tools are used, the tool shoulder rotates with the pin; thus, the material that is extruded vertically by the pin is rapidly ejected from the weld as soon as it comes in contact with the tool shoulder (owing to a higher radial speed). Thus, the material underlying the tool shoulder is highly softened causing a drastic reduction in the upsetting action exerted by the tool shoulder. Tools with stationary shoulders produce higher quality welds [18] with greater and more standardized mechanical behavior [4] as compared to welds performed by conventional tools. These improvements are due to a better stirring of the material [5] and lower variation of the plunging force during FSW [7].

So far, any investigation has been performed by controlling the plunging force during friction spot stir welding of polymer sheets. This could potentially improve the weld quality and standardization allowing a better control of the upsetting action during the cooling phase. Indeed, during this phase, different defects such as cavities and porosities, as well as thermal shrinkage, may affect the weld strength. This is due to the low pressure exerted by the tool on the underlying material [15]. This work is aimed to verify the potential advantages of plunging force control such as reduction in the amount of such defects. To this end, different levels of plunging force were used and three different tools were adopted to evaluate possible interactions between these process parameters. Morphological analysis was carried out to assess the effect of the aforementioned process parameters on development of defects. Then, single-lap shear tests were performed to evaluate how the plunging force and tool shoulder diameter influence the mechanical behavior of the welds.

2 Materials and methods

2.1 Experimental setup

Friction spot stir welding experiments were performed on 3.0 mm thick polycarbonate (PC) sheets. PC is a thermoplastic polymer characterized by good optical transparency and great mechanical properties such as high strength, high toughness, and elongation at break. For these reasons, this material is

used in different industrial fields such as optical industry, automotive, and household applications. The main mechanical and thermal properties of the investigated material were determined in a previous investigation [13]. According to that study, the material is characterized by tensile strength of 60 MPa, elongation at break of 110 %, and transition temperature of 147 °C.

The FSSW welds were made by using an instrumented CNC drilling machine equipped with a two-component piezo-electric cell (to measure the plunging force and torque) and a displacement sensor (to measure the position of the tool). The load cells were connected to a computer by means of an acquisition board. During the process, load signals were acquired and controlled by the computer by means of a feedback control system. The experimental equipment and the schematic of the control system are reported in Fig. 1a, b, respectively.

Experimental tests were performed by varying the tool dimensions. Three tools were used with varying the tool shoulder dimension D = 10, 15 and 20 mm. The pin had a cylindrical shape with a diameter d = 5 mm. This geometry was selected based on the experimental findings reported in [15]. Actually, the cylindrical pin allowed achieving higher weld strength as compared to that made by tapered pins. The tools were made of K340 stainless steel, which is heat treatable steel, turned under a CNC turning machine.

Friction spot stir welding is subdivided into distinct phases: plunging, stirring, cooling, and tool retraction, as described in Fig. 2. During the plunging phase, the tool

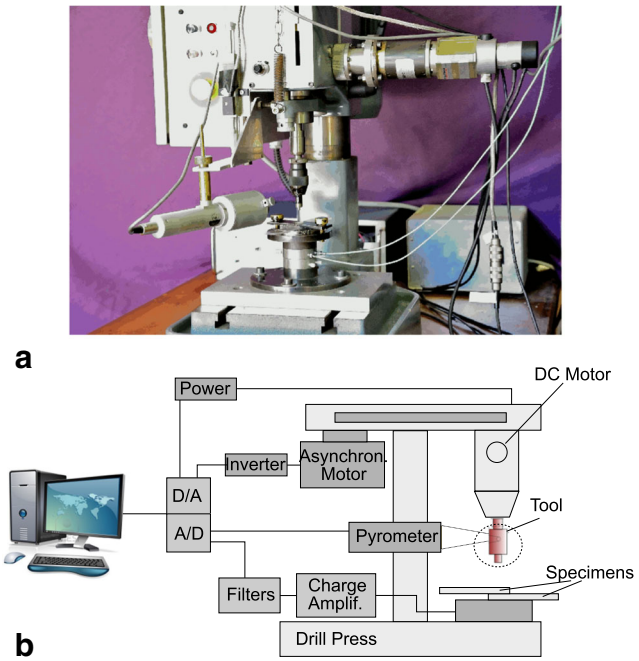

Fig. 1 **a** Experimental equipment and **b** schematic of the control system

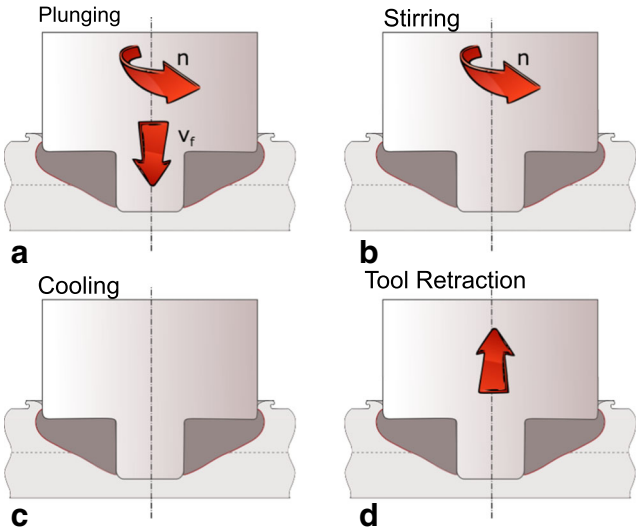

Fig. 2 Main phase of friction spot stir welding: **a** plunging, **b** stirring, **c** cooling, and **d** punch retraction

rotates and plunges the sheets until it reaches a given plunging depth. Then, the axial motion stops and the tool continues rotating (stirring) for a given duration (T_S). During this phase, a great amount of heat is produced due to frictional energy between the tool and the material. Therefore, the tool rotation is stopped to allow the material cooling. This phase is generally performed by controlling the tool position (by stopping the plunging motion). Nevertheless, because of the material ejection from the weld region, the tool is not completely in contact with the underlying material, or the stirred zone may be detached from the underlying material. This has detrimental effects on the quality of the developing weld due to low pressure that is exerted by the tool on the underlying material [20] that results in formation of defects such as cavities and porosities. The presence of such defects affects the mechanical behavior of the welds, since they reduce the extension of the weld area and promote the development of stress concentration around the defects. In this work, the cooling phase is carried out by means of a force control system that ensures a prescribed pressure being exerted on the weld. The force applied on the tool is given by product of the selected pressure P by the tool area ($D^2/4{\cdot}\pi$).

According to a series of preliminary tests, the pressure was varied in the range 0.8–1.6 MPa, as reported in Table 1. On the other hand, the other processing parameters, the plunging speed (v_f = 8 mm/min), stirring time (T_S = 15 s), cooling time (T_C = 15 s), and tool rotational speed (n = 1260 rpm), were kept constant. A full factorial experimental plan comprising 12 experimental conditions was carried out, as summarized in Table 1. The joining condition is thus codified by *Dx-y*, where x is the tool shoulder diameter and y is the control type during cooling, as reported in Table 1.

Table 1 Full factorial experimental plan: factors and levels

Level	Tool shoulder diameter, D [mm]	Control type during cooling phase (pressure [MPa])
I	10	Displacement control (DC)
II	15	Force control (FC0.8)
III	20	Force control (FC1.2)
IV		Force control (FC1.6)

2.2 Characterization of FSSW welds

The mechanical behavior of the welds was assessed by means of single-lap shear tests. The tests were performed using a universal testing machine model 322.31 by MTS under displacement control with a constant cross-head speed of 0.5 mm/min. Five repetitions for each processing conditions were performed, and the mean mechanical characteristics, shear strength F_r (calculated as the maximum load during the test) and specific strength S_s (calculated as the ratio of the shear strength to the tool area A), were determined.

$$S_s = \frac{F_r}{A} = \frac{F_r}{\pi \cdot \left(D/2\right)^2} \tag{1}$$

A schematic of the specimen is reported in Fig. 3.

The cross sections of the welds were analyzed by means of optical microscope with low magnification to highlight the differences in terms of characteristic dimensions and presence of defects among the welds performed by varying process parameters. In addition, post-mortem analysis of the welds (after the single-lap shear tests) was also carried out with similar techniques to understand the failure mode.

3 Results and discussion

Figure 4 shows the typical trends of the plunging force and torque measured during FSSW of the material using the tool with D = 10 mm. Similar trends were observed when larger tools were used (D = 15 mm and D = 20 mm). From Fig. 4a, it is evident how the load control acts. At the beginning of the cooling phase, the feedback control system determines the initial value of the plunging force; then, because of the material cooling, which results in material hardening, the load increases almost linearly up to the tool retraction phase begins.

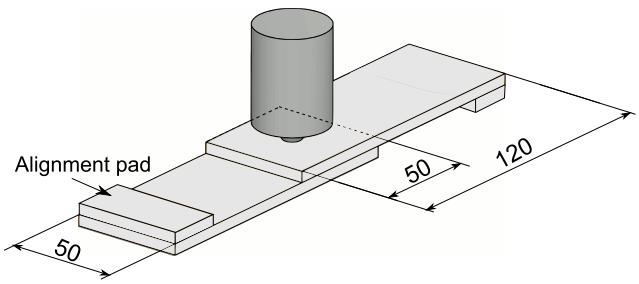

Fig. 3 Schematic of shear test specimen

As expected, the torque M_z is not influenced by the plunging condition during the cooling phase. Indeed, the plunging force was varied during the cooling phase during which the torque is negligible (since the tool rotation is stopped). Thus, the welding energy Q, which is given by Eq. 2, is not influenced by the employment of the plunging force during the cooling phase.

$$Q = \int M_z \omega \, dt \tag{2}$$

where ϖ is the tool rotation speed.

3.1 Morphology of welds

Figure 5 shows typical defects developing during FSSW of polycarbonate. The presence of such defects affects the mechanical behavior of the welds since they may act as stress raiser during loading conditions and they reduce the resistant areas of the weld. In addition, residual stress may appear in correspondence of such defects, as highlighted in Fig. 5, which reports the distribution of residual deformation shown by exploiting photo-elasticity techniques. Such stress concentration may also reduce the strength of the welds.

The aforementioned defects can be classified into two classes: defects developing at the interface between the stirred region and the surrounding material (depicted in Fig. 6a) and defects developing inside the stirred region, shown in Fig. 6b. Both defects affect the mechanical behavior of FSSW welds. Indeed, the first type of defects reduces the extension of the effective adhesion area between the base material and the stirred zone. These defects are due to thermal shrinkage and low pressure exerted by the tool during the cooling phase of FSSW process owing to partial material ejection from the weld area. After the stirring phase, a clearance may exist between the stirred zone and the underlying material. On the other hand, the second type of defect may facilitate the onset of stress concentration and reduction in the resistant area during loading conditions. These defects are due to inclusion of air during the plunging phase, thermal shrinkage during the cooling phase, and moisture absorption. Indeed, polycarbonate absorbs moisture at high rate that tends to form vapor above 120 °C and the vapor expansion creates bubbles in the weld.

The onset of these defects was studied in a number of investigations and may be reduced under certain process conditions. Mendes et al. [16] observed that in friction stir welding, high levels of heat (produced by high tool rotation speeds and low transverse speeds) may reduce or even avoid the development of such defects. The adoption of low tool

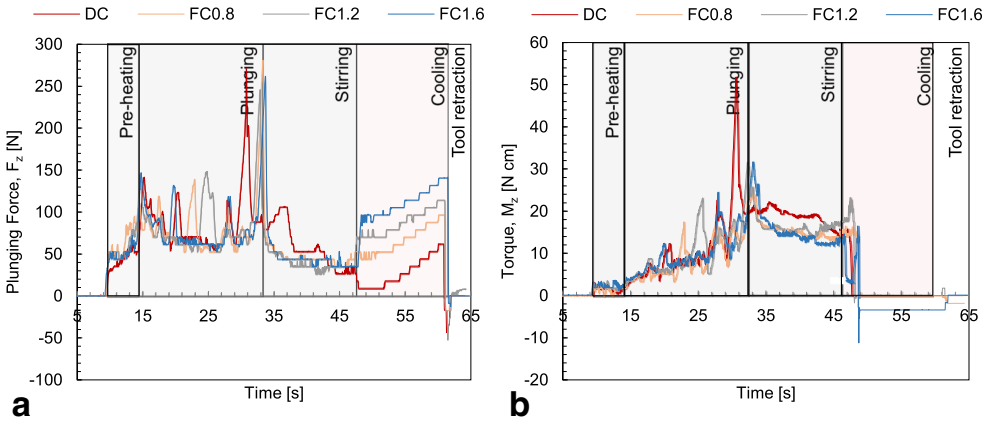

Fig. 4 Trends of the **a** plunging force and **b** torque measured during friction spot stir welding varying the plunging conditions during cooling phase (D = 10 mm)

rotation speed promotes the formation of cavities since the heat transferred is insufficient to establish the bonding of material plastically deformed by the tool. On the other hand, the presence of porosities was mainly addressed to the air entrapped in the weld because of insufficient material flow, thermal shrinkage, trapped air, or even structural changes of the polymer, as reported in [19].

Figure 7 compares the cross sections of welds performed under displacement (a) and force control (b) using the punch with D = 10 mm. As can be inferred, the first weld, depicted in Fig. 7a, shows all typical defects of FSSW polymer welds. Here, the stirred zone can be clearly identified by the presence of defects at the interface between the stirred region and the underlying (base) material. Comparing Fig. 7c, d, which were taken with higher magnification, a higher upsetting action allowed by the force control can be appreciated.

The weld made under plunging force control showed a high transparency in the stirred region that suggests a closure of the defects developed between the stirred region and surrounding material. Thus, using certain plunging force on the tool during the cooling phase ensured a close contact between the stirred region and the underlying material during the cooling phase. In addition, the material of the stirred region is highly softened because of the high temperature leading to a low flow stress. Thus, the defects at the interface can be easily

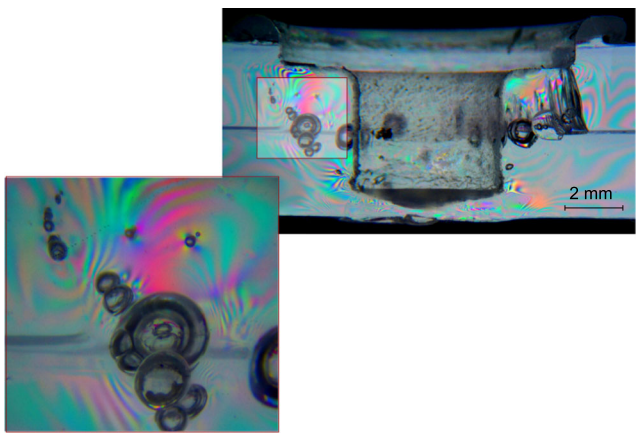

Fig. 5 Residual stress concentrating around defects observed by photoelasticity techniques

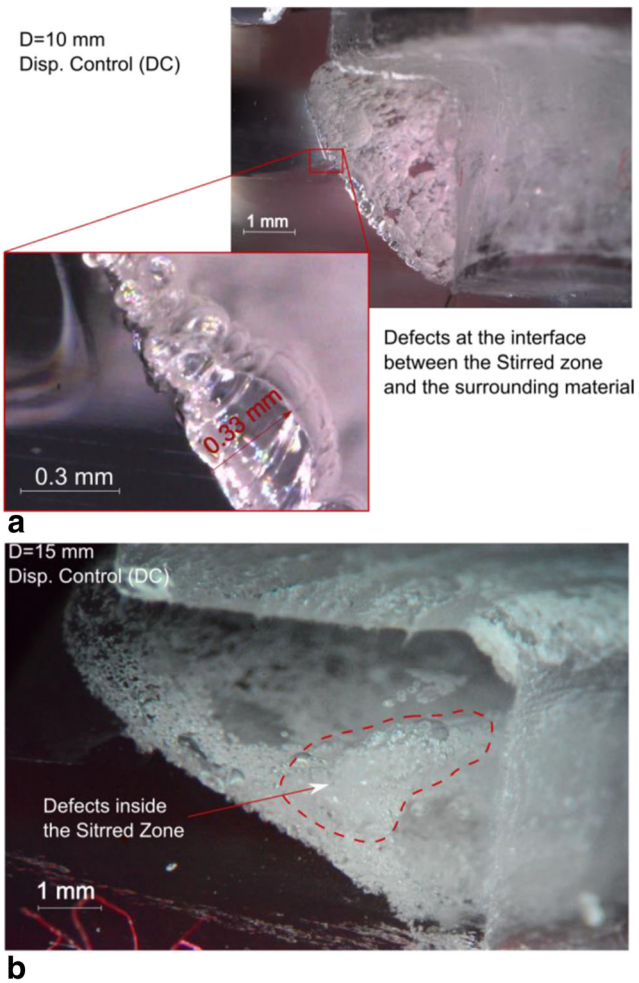

Fig. 6 Defects developing at **a** the interface between stirred zone and surrounding material and **b** inside the stirred zone

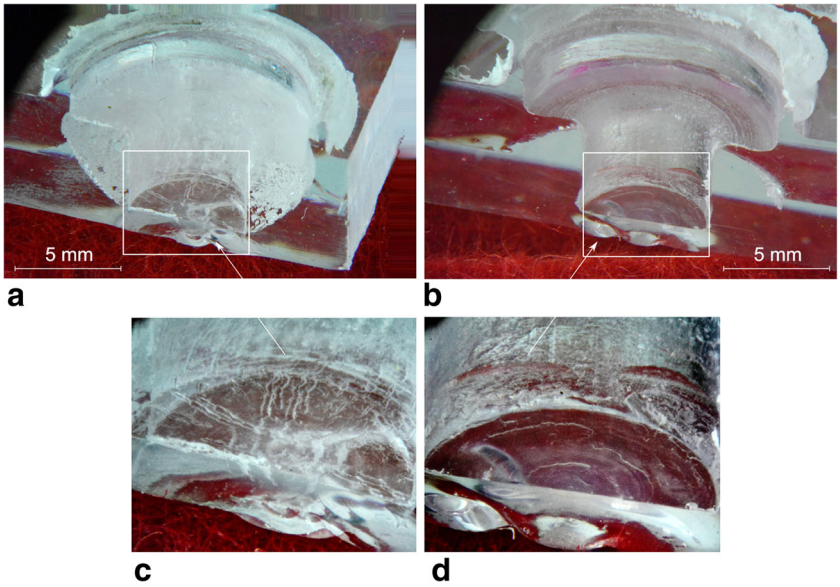

Fig. 7 Cross section of FSS welds performed under **a** displacement control and **b** force control (d = 5 mm, D = 10 mm)

deformed and cavities can be avoided by the employment of the plunging force at the beginning of the cooling phase.

To better understand how the force control influences the material flow and defects development, a series of pictures were taken during the FSSW process, as reported in Fig. 8, exploiting the transparency of the polycarbonate.

During the stirring phase, a part of the material is ejected from the weld because of the tool plunging and the centrifugal forces acting on softened material. During the cooling phase, a clearance may exists between the stirred zone (SZ), which rotated with the tool, and the surrounding material (SM). The thickness of the clearance may increase owing thermal shrinkage (during cooling phase when displacement control is adopted). This leads to two disadvantages: high temperature gradients between the SZ and the SM and poor compressive stress that result in weak adhesion and formation of defects at the interface. In some cases, such weak adhesion may determine the early separation of the SZ from the SM during service life [15].

On the contrary, when the force control is adopted, the close contact between the SZ and the SM is ensured even during the cooling phase allowing a better adhesion between the SZ and SM. This results in more homogeneous temperature distribution and partial or complete closure of porosities at the SZ-SM interface. The plunging force control involves beneficial effects on the mechanical behavior of the welds that fail by shear rather than separation of the stirred zone from the lower sheet. Figure 9 shows the cross sections of welds made by the tool with the smaller tool shoulder (D = 10 mm). As it can be inferred, the welds made by force control were almost free from defects at the SZ-SM interface; however, some defects inside the stirred region were still observable. Similar characteristics were shown by the welds made by larger tools (D = 15 mm and D = 20 mm).

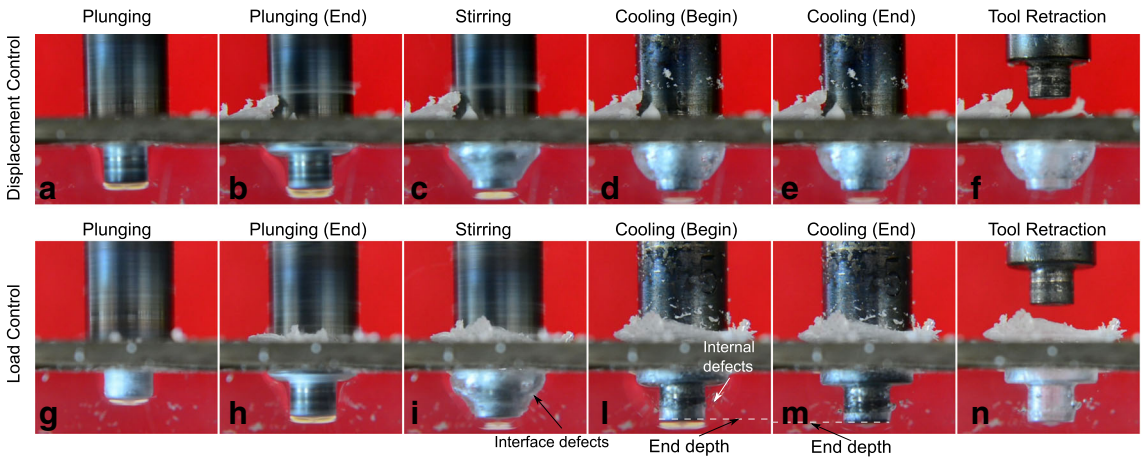

Fig. 8 Material flow during FSSW using **a**–**f** displacement control and **g**–**n** load control (P = 1.2 MPa)

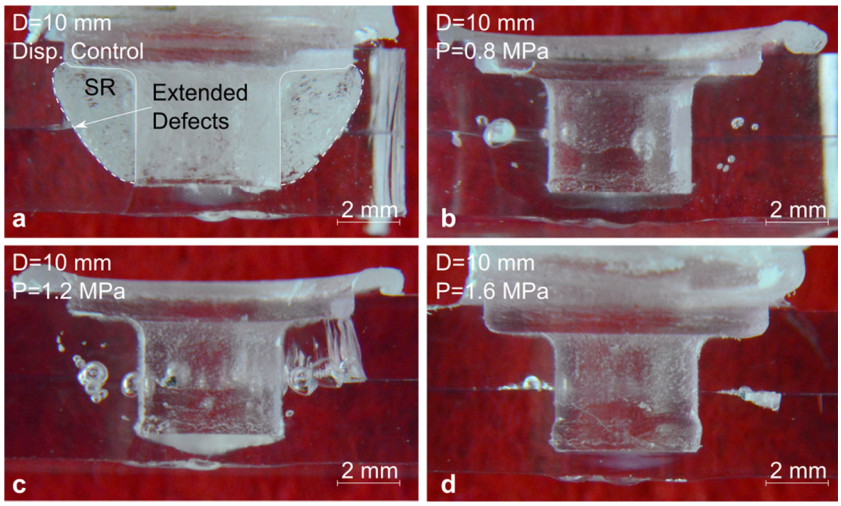

Fig. 9 Cross sections of specimens made by tool with D = 10 mm using different plunging conditions during cooling phase

3.2 Dimensional analysis of welds

The mechanical behavior of FSS welds is mainly determined by the strength of the material, presence of aforementioned defects, geometry of the welds, and residual stress. The occurrence of the different failure modes depends on the characteristics dimensions of the FSSW welds [15]: the weld area A_{weld}, the interface area between the stirred zone and the upper sheet A_{up}, and the interface area of the stirred zone with the lower sheet A_{lo}. These areas are reported in Fig. 10. Welds showing small values of A_{weld} are likely to fail by shear fracture, while low values of A_{up} and A_{lo} are likely to result in failure by separation of the stirred zone from the upper and lower sheets, respectively.

During the single-lap shear tests performed in this investigation, a further failure mode was observed: tearing of the upper sheet. This failure mode was due to excessive reduction of the residual thickness of the upper sheet in correspondence of the stirred region. Thus, to understand the influence of the plunging force applied during the cooling phase, the main dimension of the welds was examined. Figure 11b shows the variation of the residual thickness of the upper sheet h_R with varying the pressure P and punch shoulder diameter D. From the trends reported in Fig. 11, it is evident that for D = 10 mm, the residual thickness of the upper sheet h_R holds almost constant up to P = 1.2 MPa. Further increase in the applied pressure (P = 1.6 MPa) resulted in steep reduction in h_R; under such conditions; the plunging pressure is likely to overcome the yield strength of the PC and frictional force at the tool-shoulder/material interface. On the other hand, for larger tools (D = 15 mm and D = 20 mm), any significant variation of h_R was observed even for P = 1.6 MPa. This difference was

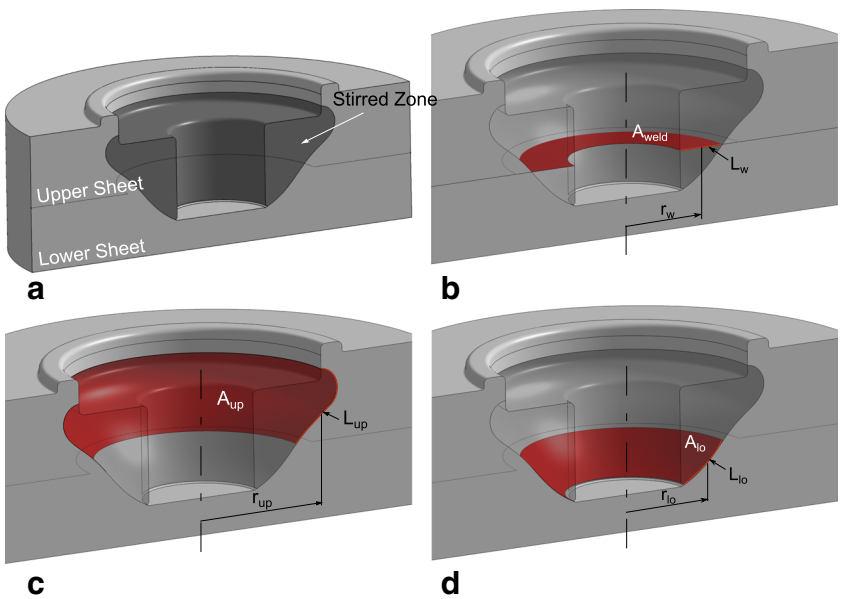

Fig. 10 Critical regions of FSSW of polymers [15]

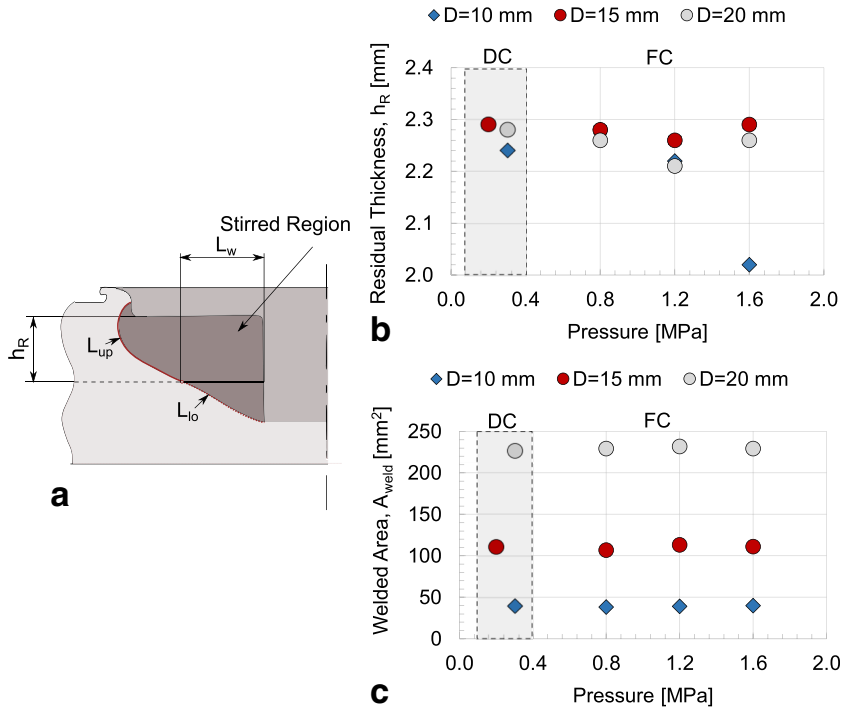

Fig. 11 **a** Schematic of characteristic dimensions of a FSSW weld; variation of **b** residual thickness and welded area with plunging force and tool diameter

addressed to higher frictional forces developing at the material/tool-shoulder interface that over-constrained the PC material flow.

On the other hand, A_{weld} was negligibly influenced by the plunging force applied during the cooling phase, while it was mainly determined by the tool shoulder diameter, as shown in Fig. 11c.

3.3 Mechanical behavior of the welds

The variation of the nominal shear strength S_s, calculated as the ratio of the maximum load F_r (recorded during single-lap shear tests) to the tool area A, varying the plunging force and tool shoulder diameter D is reported in Fig. 12. S_s decreases almost linearly with the increase in the tool shoulder D, in agreement with the experimental findings reported in [15]. This is due to the quadratic increase of A with D (L_w shows a linear increase with D) and an almost linear increase of F_r with D.

For the welds made by the tools with D = 10 mm and D = 20 mm, S_s shows a maximum for an intermediate level of pressure (P = 1.2 MPa). Thus, in these welds, the control of the plunging force allowed improving the shear strength as compared to welds made by position control. However, excessive increase in the plunging force resulted in decreasing in shear strength.

The welds made by the tool with D = 10 mm showed the highest shear strength, which reached 25 MPa under displacement control, while S_s increased by almost 37 % (up to almost 34.5 MPa). Thus, the shear strength of the weld under optimal condition (D = 10 mm and P = 1.2 MPa) yields that of the base material calculated using the von Mises criterion $\tau_s = \sigma_s/\sqrt{3} = 60/1.732 = 34.6$ MPa, where τ_s and σ_s are the shear strength and tensile strength of the base material, respectively.

On the other hand, the shear strength of the welds made by the tool with D = 15 mm was slightly influenced by P. These different behavior was addressed to the different failure mode of these welds, which failed by brittle fracture in the lower sheet. On the other hand, the welds made by the smaller tool shoulder (D = 10 mm) failed by shear fracture, and those made by the largest tool diameter (D = 20 mm) failed by tearing of the upper sheet. These three types of failure modes are reported in Fig. 13.

Tearing of the upper sheets consisted of stress localization and thinning of the upper sheet material that was in contact with the tool shoulder during the welding process, as shown in

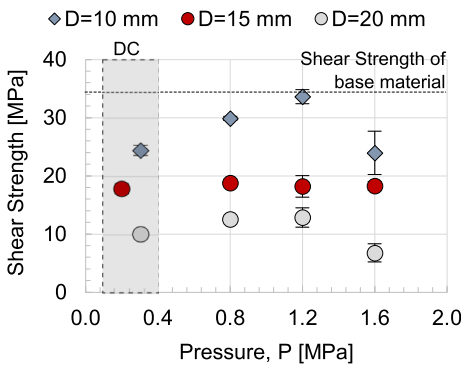

Fig. 12 Variation of the nominal shear strength of the welds with varying the plunging force during cooling phase

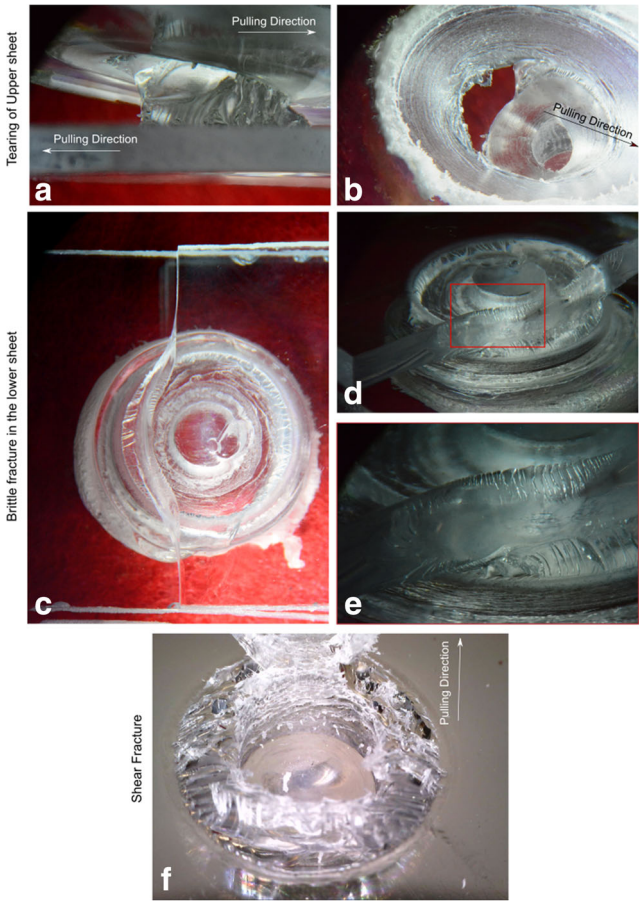

Fig. 13 Failure modes of FSSW welds: **a**–**b** Tearing of upper sheet; **c**–**e** brittle fracture in the lower sheet and **f** shear fracture

Fig. 13a, b. The welds failing by tearing of the upper sheet (those made by the tool with $D = 20$ mm) were characterized by a good adhesion of the stirred zone with the underlying material and the presence of a reduced number of defects inside the stirred region. Similarly, the welds failing by shear fracture (those made by the tool with $D = 10$ mm) were characterized by a few number of defects within the stirred region. In this case, the extension of the welded area was smaller than in previous ones, thus the critical parameter was A_{weld}. In both the aforementioned welds, the fracture developed progressively without steep variations of the load until the complete separation of the sheets. In addition, these welds allowed absorbing high amount of energy during single-lap shear tests. On the other hand, in the welds made by the tool with $D = 15$ mm, brittle fracture in the lower sheets was observed. Unlike the previous ones, the failure developed almost instantly. This fracture mode was due to the larger amount of defects within the stirred region which acted as stress raiser, as shown in Fig. 6b. Thus, these welds did not benefit of the force control because the failure was mainly due to the defects inside the stirred region, which were only marginally reduced with the adoption of the force control.

Figure 14 compares the load-displacement curves of welds made with varying the tool shoulder diameter and the plunging force during cooling phase. These curves confirm the abovementioned behavior and the influence of process parameters and suggest that for the welds made by tools with $D = 10$ mm and $D = 20$ mm, the force control allows to improve also the absorbed energy, while negligible differences are observable when comparing the curves D15-DC and D15-FC0.8, which were performed with the tool with $D = 15$ mm under displacement and force control (0.8 MPa), respectively. In addition, the stiffness of the welds made by the tool with $D = 20$ mm and load control (D20-FC0.8) is higher than that of the welds made by the same tool under displacement control (D20-DC). This suggests that the closure of the porosities at the interface increases the adhesion area (between the stirred zone and the underlying material) leading to a stiffer behavior.

In the welds made by the tool with $D = 10$ mm, the adoption of the force control produces a similar effect of that achieved by increasing the stirring time, as reported in [20]. In the first case, the increase in the mechanical behavior is due to a better adhesion of the stirred zone to the underlying material (quality of the weld), while in the latter case, such an increase is due to a larger adhesion area.

From a process point of view, despite of the development of the FSSW with force control requires the employment of a feedback control system (which is commonly available of friction spot stir welding machines) and a load cell to measure and control the plunging force, the force control offers different advantages with respect to the increase in the stirring time including reduction of defects, reduction in energy spent during the welding operation, and reduction in the processing time.

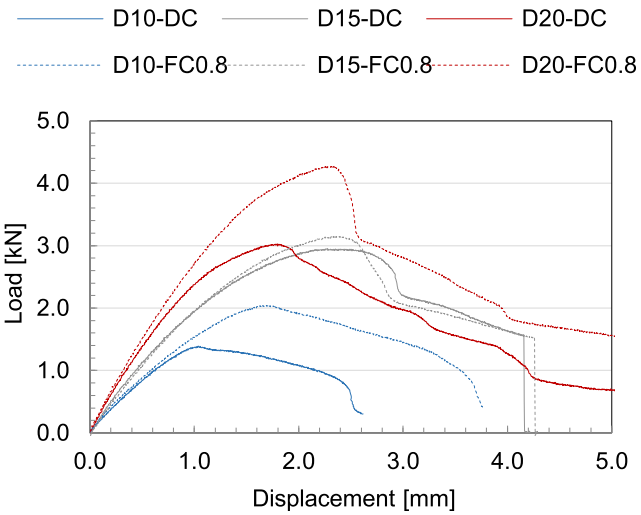

Fig. 14 Load-displacement curves of welds made by displacement and force control and different tool shoulders

4 Conclusions

The present work investigated the effect of controlling the plunging force during the cooling phase of friction spot stir welding of polycarbonate sheets. To this end, the mechanical behavior of the welds made by different tools performed under displacement and force control was compared. Accordingly, geometrical and morphological analysis of the welds were performed to understand the influence of the process parameters on the strength of the welds. The main results are reported as follows:

- the force control during the cooling phase allowed to improve the mechanical behavior of the welds made by the tools that failed by shear fracture (with tool shoulder diameter D = 10 mm) and tearing of the upper sheet (D = 20 mm), while it had negligible influence for the mechanical behavior of welds that failed by brittle fracture in the upper sheet (D = 15 mm);
- the improvement in the mechanical behavior of the welds is mainly due to the closure of the porosities and cavities developing at the interface of the stirred zone surrounding regions. On the other hand, the amount of defects inside the stirred zone is negligibly influenced by the force control;
- under optimal processing conditions (D = 10 mm and P = 1.2 MPa), the force control allowed to increase the strength of almost 37 % with respect to the welds made by force control (with the same tool) without increasing the required welding energy or increasing the welding time. Under such conditions, the nominal shear strength reached 34.5 MPa, which yields that of the base material;
- the employment of load control during the cooling phase of FSSW process does not involve any increase in welding energy and welding time; thus, it represents a "environment-friendly" improvement of the process without affecting its productivity.

Acknowledgments The authors would also like to thank Mr. Giuseppe Organtini (DIIIE—University of L'Aquila) for the contribution during the setup and conduction of the experimental tests. The authors would also like to thank Eng. Silvio Genna from the University of Naples (CIRTIBBS) for his support during fractography analysis.

References

1. Abibe AB, Sônego M, dos Santos JF, Canto LB, Amancio-Filho ST (2016) On the feasibility of a friction-based staking joining method for polymer–metal hybrid structures. Mater Des 92:632–642
2. Acherjee B, Kuar AS, Mitra S, Misra D (2014) Laser transmission welding of polycarbonates: experiments, modeling, and sensitivity analysis. Int J Adv Manuf Technol 78:853–861
3. Aden M, Mamuschkin V, Olowinsky A (2015) Influence of carbon black and indium tin oxide absorber particles on laser transmission welding. Opt Laser Technol 69:87–91
4. Azarsa E, Mostafapour Asl A, Tavakolkhah V (2012) Effect of process parameters and tool coating on mechanical properties and microstructure of heat assisted friction stir welded polyethylene sheets. Adv Mater Res 445:765–770
5. Bagheri A, Azdast T, Doniavi A (2013) An experimental study on mechanical properties of friction stir welded ABS sheets. Mater Des 43:402–409
6. Bilici MK, Yukler AI (2012) Effects of welding parameters on friction stir spot welding of high density polyethylene sheets. Mater Des 33:545–550
7. Eslami S, Ramos T, Tavares PJ, Moreira PMGP (2015) Effect of friction stir welding parameters with newly developed tool for lap joint of dissimilar polymers. Procedia Eng 114:199–207
8. Gao J, Li C, Shilpakar U, Shen Y (2015) Improvements of mechanical properties in dissimilar joints of HDPE and ABS via carbon nanotubes during friction stir welding process. Mater Des 86:289–296
9. Gao J, Li C, Shilpakar U, Shen Y (2016) Microstructure and tensile properties of dissimilar submerged friction stir welds between HDPE and ABS sheets. Int J Adv Manuf Technol. doi:10.1007/s00170-016-8539-y
10. Hoseinlaghab S, Mirjavadi SS, Sadeghian N, Jalili I, Azarbarmas M, Besharati Givi MK (2015) Influences of welding parameters on the quality and creep properties of friction stir welded polyethylene plates. Mater Des 67:369–378
11. Husain IM, Salim RK, Azdast T, Hasanifard S, Shishavan SM, Eungkee Lee R (2015) Mechanical properties of friction-stir-welded polyamide sheets. Int J Mech Mater Eng 10:18
12. Lambiase F, Genna S (2017) Laser-assisted direct joining of AISI304 stainless steel with polycarbonate sheets: thermal analysis, mechanical characterization, and bonds morphology. Opt Laser Technol 88:205–214
13. Lambiase F, Paoletti A, Di Ilio A (2015) Mechanical behaviour of friction stir spot welds of polycarbonate sheets. Int J Adv Manuf Technol 80:301–314
14. Lambiase F, Paoletti A, Di Ilio A (2016a) Effect of tool geometry on loads developing in friction stir spot welds of polycarbonate sheets. Int J Adv Manuf Technol. doi:10.1007/s00170-016-8629-x
15. Lambiase F, Paoletti A, Di Ilio A (2016b) Effect of tool geometry on mechanical behavior of friction stir spot welds of polycarbonate sheets. Int J Adv Manuf Technol. doi:10.1007/s00170-016-9017-2
16. Mendes N, Loureiro A, Martins C, Neto P, Pires JN (2014a) Effect of friction stir welding parameters on morphology and strength of acrylonitrile butadiene styrene plate welds. Mater Des 58:457–464
17. Mendes N, Neto P, Simão MA, Loureiro A, Pires JN (2014b) A novel friction stir welding robotic platform: welding polymeric materials. Int J Adv Manuf Technol 85:37–46
18. Mostafapour, A., Azarsa, E., 2012. A study on the role of processing parameters in joining polyethylene sheets via heat assisted friction stir welding: investigating microstructure, tensile and flexural properties. Int J Phys Sci 7
19. Oliveira PHF, Amancio-Filho ST, dos Santos JF, Hage E (2010) Preliminary study on the feasibility of friction spot welding in PMMA. Mater Lett 64:2098–2101
20. Paoletti A, Lambiase F, Di Ilio A (2016) Analysis of forces and temperatures in friction spot stir welding of thermoplastic polymers. Int J Adv Manuf Technol 83:1395–1407
21. Pirizadeh M, Azdast T, Rash Ahmadi S, Mamaghani Shishavan S, Bagheri A (2014) Friction stir welding of thermoplastics using a newly designed tool. Mater Des 54:342–347
22. Rodríguez-Vidal E, Quintana I, Gadea C (2014) Laser transmission welding of ABS: effect of CNTs concentration and process parameters on material integrity and weld formation. Opt Laser Technol 57:194–201

23. Sadeghian N, Besharati Givi MK (2015) Experimental optimization of the mechanical properties of friction stir welded acrylonitrile butadiene styrene sheets. Mater Des 67:145–153
24. Vijendra B, Sharma A (2015) Induction heated tool assisted friction-stir welding (i-FSW): a novel hybrid process for joining of thermoplastics. J Manuf Process 20:234–244
25. Yusof F, Muhamad M, Moshwan R, Jamaludin M, Miyashita Y (2016) Effect of surface states on joining mechanisms and mechanical properties of aluminum alloy (A5052) and polyethylene terephthalate (PET) by dissimilar friction spot welding. Metals 6:101